nature electronics

REVIEW ARTICLE

https://doi.org/10.1038/s41928-020-0400-5

Non-reciprocal electronics based on temporal modulation

Aravind Nagulu[1], Negar Reiskarimian[1,2,3] and Harish Krishnaswamy[1]✉

In general, reciprocity requires that signals travel in the same manner in both forward and reverse directions. It governs the behaviour of the majority of electronic circuits and components, imposing severe restrictions on how they operate. Components that violate reciprocity, such as gyrators, isolators and circulators, are, however, of use in many different electronic applications. Non-reciprocal electronic components have typically been implemented using ferrites, but such magnetic materials cannot be integrated in modern semiconductor fabrication processes and magnetic non-reciprocal components remain bulky and expensive. Creating non-reciprocal components without the use of magnetic materials has a long history, but has recently been reinvigorated due to advancements in semiconductor technology. Here we review the development of non-reciprocal devices and the development of non-magnetic non-reciprocal electronics, focusing on devices based on temporal modulation, which arguably exhibit the greatest potential. We consider approaches based on temporal modulation of permittivity and conductivity, as well as hybrid acoustic–electronic components, which have applications including high-power transmitters for communications, simultaneous transmit and receive radars, and full-duplex wireless radios. We also explore superconducting non-reciprocal components based on temporal modulation of permeability for potential applications in quantum computing and consider the key future challenges in the field.

The principle of reciprocity as an underlying symmetry spans various branches of physics, including electromagnetics and optics, acoustics, thermodynamics, and elastodynamics, and its study has a rich history that dates back to, amongst others, the work of Green, Rayleigh, Helmholtz, Lorentz, Carson, Onsager and Casimir[1–8]. In electromagnetic wave propagation, reciprocity essentially implies that wave propagation remains unchanged if the source point and observation point are interchanged. The implications of reciprocity are widespread in electronics. It is reciprocity, for instance, that enables a microwave or optical power splitter to function as a power combiner when used in the reverse direction, and causes antennas to radiate in the same manner as they receive[9].

For a linear network with a finite number of ports, reciprocity implies that the scattering matrix S of the network satisfies the symmetry condition $S^{T} = S$, where S^{T} is the transpose of matrix S. Non-reciprocity should not be confused with asymmetric transmission in multi-mode structures[10,11]. Different modes at the same physical port can be formulated as unique ports in a scattering matrix representation, and if the scattering matrix is symmetric, the multi-mode structure is reciprocal. An example of an asymmetric multi-mode structure that is still reciprocal is a structure that features one-way mode conversion[11]: mode A incident at port 1 is strongly converted to mode B at port 2, but when mode A is incident at port 2, it is not converted to mode B at port 1. Such a structure can still be reciprocal as long as mode B incident at port 2 is similarly strongly converted back to mode A at port 1.

The Lorentz reciprocity theorem for electromagnetism requires that any linear and time-invariant medium with symmetric permittivity and permeability tensors be reciprocal. In 1948, Tellegen proposed the non-reciprocal gyrator as the fifth fundamental circuit element, after the resistor, capacitor, inductor and transformer[12]. The significance of the gyrator is that, along with the other four reciprocal fundamental circuit elements, it can be used to synthesize any arbitrary non-reciprocal circuit. Shortly after, the first gyrator was built using magnetic materials and exploiting the Faraday effect[13], and this approach remains the dominant means of building non-reciprocal components.

Non-reciprocal components are of use today in many applications, including high-power wireless base-station transmitters, simultaneous-transmit-and-receive (STAR) radar, full-duplex wireless radios and quantum computing implementations. However, despite efforts to integrate magnetic materials such as ferrites with semiconductor integrated-circuit fabrication technologies[14], which have become the basis for virtually all forms of low-cost electronics, such integration remains challenging. Consequently, magnetic non-reciprocal components tend to be bulky and expensive devices, and their deployment tends to be restricted to scenarios that are free of stringent size, weight and cost requirements. The ability to implement non-magnetic non-reciprocal components has the potential to revolutionize these applications, provided the implementations can meet the stringent performance requirements.

In this Review Article, we examine the implementation of non-magnetic non-reciprocal electronics with a focus on devices based on temporal modulation, which arguably show the greatest promise from a performance perspective. We first consider the applications of non-reciprocal components and their associated performance requirements, and non-reciprocal electronics based on active transistors or nonlinearity. We then consider approaches based on temporal modulation of permittivity and conductivity, as well as hybrid acoustic–electronic components. Finally, we explore superconducting temporally modulated components for emerging quantum computing applications and explore future research directions for the field.

[1]Department of Electrical Engineering, Columbia University, New York, NY, USA. [2]Microsystems Technology Laboratories, Massachusetts Institute of Technology, Cambridge, MA, USA. [3]Department of Electrical Engineering and Computer Science, Massachusetts Institute of Technology, Cambridge, MA, USA. ✉e-mail: harish@ee.columbia.edu

Applications and requirements of non-reciprocal components

Two common non-reciprocal components are the isolator and the circulator, whose scattering parameters (S_{ISO} and S_{CIRC}, respectively) are given below.

$$S_{ISO} = \begin{bmatrix} 0 & 0 \\ 1 & 0 \end{bmatrix}, S_{CIRC} = \begin{bmatrix} 0 & 0 & 1 \\ 1 & 0 & 0 \\ 0 & 1 & 0 \end{bmatrix} \quad (1)$$

As can be seen from the *S* parameters, the isolator is a matched two-port non-reciprocal component that allows lossless transmission in the forward direction, but no transmission in the reverse direction. Isolators are used to protect high-power wireless transmitters from back reflections from the antenna. Back reflections can increase the output voltage swing of the transmitter, potentially inducing device breakdown in the power amplifier. The circulator is a matched three-port non-reciprocal component that allows lossless transmission in a clockwise (or counter-clockwise) rotary sense between its three ports, but no transmission in the reverse rotary sense. Circulators are used to interface a transmitter and a receiver to a shared antenna, allowing them to transmit and receive simultaneously at the same frequency. This is critical for emerging full-duplex wireless applications[15], as well as STAR radar. Although reciprocal alternatives exist for this functionality, such as hybrid couplers or electrical-balance duplexers[16], which feature simultaneous transmission between two isolated ports and a third port, the fact that a three-port passive reciprocal network cannot be lossless and matched at all ports implies that the transmission will feature a minimum of 3 dB loss. Quantum computing implementations based on superconducting technology also extensively use circulators and isolators at cryogenic temperatures, with the size and cost of magnetic implementations currently a substantial bottleneck in the ability to integrate multiple qubits in a single dilution fridge[17].

While the performance requirements vary across these different applications, the most important metrics are insertion loss, power handling, bandwidth, isolation, noise performance (quantified by noise figure), nonlinear distortion performance (quantified by the input- or output-referred third-order intercept point or IIP3) and size. Lower insertion losses are of course desirable across all applications. The insertion losses of microwave magnetic isolators and circulators are often below 1 dB (ref. [18]), a challenging metric to achieve for emerging non-magnetic implementations. Most methods for temporal modulation are associated with some loss, although the amount of loss varies depending on the method. It may be argued that non-magnetic non-reciprocal components can be a viable alternative at slightly higher loss levels (perhaps 2 dB) as the ability to integrate these components on a semiconductor chip allows for other benefits, such as co-design opportunities with the rest of the electronics. For instance, time-modulated circulators have been demonstrated that absorb the functionality of the antenna tuner and the down-conversion mixer of a wireless receiver[19]. Therefore, the loss of such a circulator has to be compared with the cascaded loss of a conventional antenna tuner, magnetic circulator and down-conversion mixer. At the same time, it can also be argued that the loss level should be below 3–4 dB as, at these levels, reciprocal alternatives such as hybrid couplers and electrical balance duplexers become viable, while requiring no modulation and being extremely linear.

Power handling is another challenging metric — microwave magnetic isolators and circulators can handle tens to hundreds of watts of input power[18], while the best time-modulated non-reciprocal components currently achieve power handling of the order of a few watts[20]. Such power handling allows them to be considered for commercial handheld wireless devices, where the transmit power is around a watt for cellular applications and of the order of hundreds of milliwatts for WiFi applications. However, high-power base-station transmitters and transmitters used in defence applications use power levels of tens of watts or more, and therefore will still require magnetic non-reciprocal components for the immediate future.

Bandwidth is also application dependent. Commercial wideband cellular and WiFi applications use several tens of MHz of bandwidth at radio frequencies below 6 GHz, while defence applications can use bandwidths of hundreds of MHz or more. Emerging commercial '5G' millimetre-wave applications at 28 GHz and 39 GHz are exploring bandwidths as wide as hundreds of MHz to 1 GHz. Recently reported time-modulated non-reciprocal components show promise in achieving, and indeed exceeding, these operating bandwidths[20–23].

Linear, time-invariant passive devices exhibit a noise figure that is equal to their insertion loss. Essentially, this means that the thermal noise level is unchanged between the input and output ports, and the only degradation in signal-to-noise ratio is due to the reduction in the desired signal power level due to the insertion loss. It is desirable that time-modulated non-reciprocal components exhibit similar behaviour, but without careful design, the phase noise of the modulating signal can degrade the noise performance[24]. More recently, the design approaches required to mitigate such noise degradation have been understood[20,21], and noise figures that are equal to insertion loss have been reported. However, an unresolved problem is the noise performance at a certain port of the component while another port is simultaneously excited by a powerful signal. Such a scenario arises in circulators for full-duplex wireless, where the noise performance from the antenna port to the receiver port must be exemplary while the transmitter port is simultaneously being excited. In such a scenario, a phenomenon called 'reciprocal mixing' occurs, where the transmitter signal mixes with the phase noise of the modulation signal to degrade the noise performance at the receiver port[20]. Mitigation of this reciprocal-mixing effect still remains an open research problem.

It must be emphasized that all of these metrics fundamentally trade off with size. For instance, achieving higher power handling within a smaller volume is fundamentally challenging irrespective of the implementation technology, due to increasing field strength within smaller dimensions for the same power level. While the state-of-the-art non-magnetic non-reciprocal components trail their magnetic counterparts in most performance metrics, they are substantially more compact, down to chip scale (a few millimetres on each dimension)[20,21]. Furthermore, the gap in performance metrics is steadily shrinking, due to the active nature of the research area, promising a future where these non-magnetic non-reciprocal components are widely deployed in a variety of applications.

Non-reciprocity based on active transistors or nonlinearity

In order to combat the size, weight and cost of ferrite-based components, some of the first attempts to realize non-magnetic non-reciprocal components relied on the inherent non-reciprocity of active voltage- or current-biased transistors, which offer gain in the forward direction and isolation in the reverse direction, and are of course readily available in semiconductor integrated circuits. One of the earliest works was reported in ref. [25], which exploited a circular connection of active transistors, as shown in Fig. 1c. As semiconductor integrated-circuit fabrication has advanced over the last several decades, investigations of active non-reciprocal components have continued[26]. This concept has also been extended to metamaterials that embed active transistors to realize non-reciprocal wave propagation in a medium (Fig. 1b)[27]. However, the biasing is fundamentally associated with noise and nonlinear distortion when the desired signal becomes comparable to the bias level[28]. While these issues can be somewhat mitigated through the use of high-performance transistor technologies, such as gallium arsenide

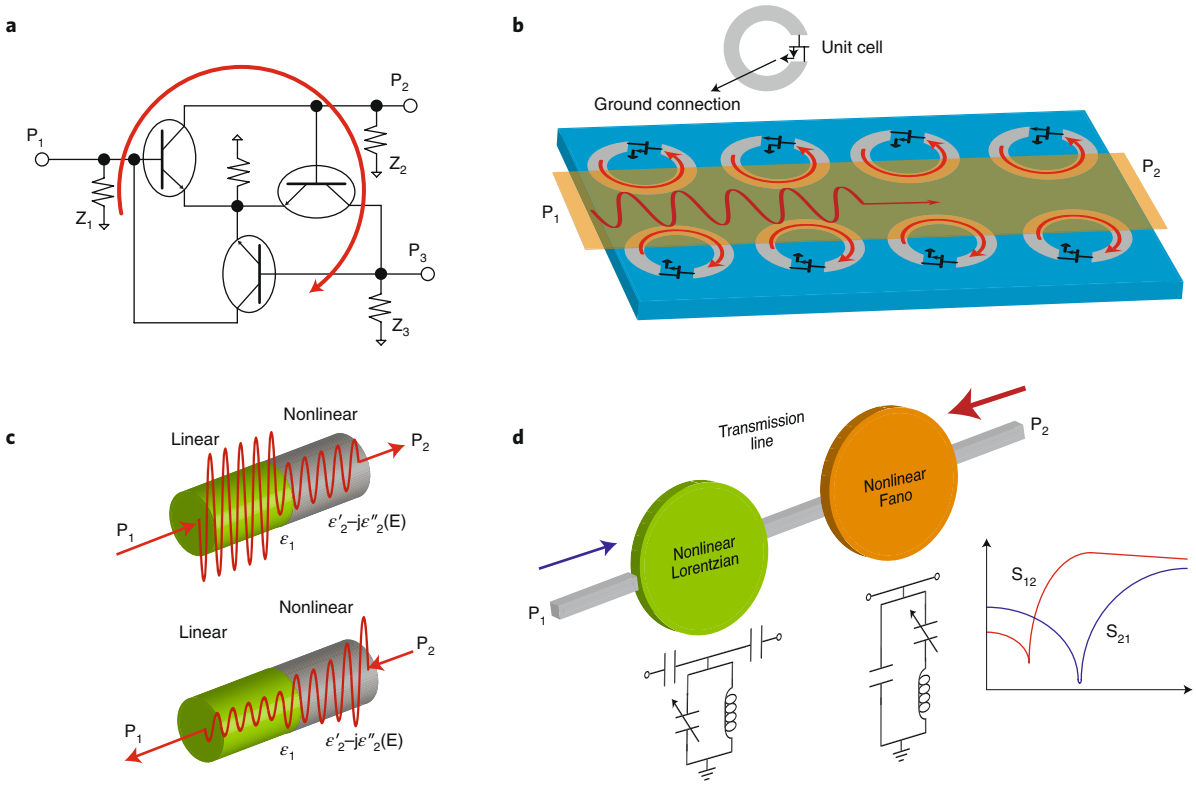

Fig. 1 | Non-reciprocity based on active transistors or nonlinearity. a, A non-magnetic non-reciprocal circulator based on a circular connection of active-biased transistors where Z_1, Z_2 and Z_3 represent the collector loads of the active transistors[25]. Device ports are indicated by P. **b**, Metamaterial supporting non-reciprocal wave propagation based on embedded active transistors. Each unit cell consists of a ring resonator loaded with a transistor switch[27]. **c**, Principle of operation of nonlinear isolators within a cascade of two media where ε_1 represents the permittivity of the linear medium, and ε'_2 and ε''_2 represent the linear and non-linear components of the permittivity of the non-linear medium, respectively. **d**, A nonlinear isolator based on a cascade of a nonlinear Lorentzian resonator and a nonlinear Fano resonator[33]. Inset: the scattering parameters of the nonlinear isolator, representing low loss from port 2 to port 1 (S_{12}) and high isolation from port 1 to port 2 (S_{21}).

(GaAs) and gallium nitride (GaN), active non-reciprocal components based on low-cost complementary metal–oxide–semiconductor (CMOS) technologies exhibit limited dynamic range, and find limited utility in applications where low-noise and low-distortion operation are critical, such as communication, radar and quantum signal processing.

Reciprocity can also be broken through the use of nonlinear media or circuits that exhibit spatial asymmetry. Such approaches have been widely explored at optical frequencies exploiting the rich body of research on nonlinear photonics[29–31] as well as at radio frequencies and with microwaves[32–35]. While many different approaches have been investigated, the operation of such nonlinear isolators generally relies on the fact that the response of a nonlinear medium depends on the amplitude of the signal propagating through it. Generally, nonlinearity in media, devices and circuits tends to be compressive, implying that more powerful signals undergo more severe attenuation. The spatial asymmetry implies that signals incident from one side enter the nonlinear region with greater amplitude, undergoing more attenuation, while signals entering from the other side enter the nonlinear region with lesser amplitude, and suffer less attenuation (Fig. 1c). However, the fundamental challenge with such approaches is that non-reciprocity is only exhibited over a limited range of signal power levels. There have been interesting recent efforts towards extending the range of supported signal levels, such as the work in ref. [33] and Fig. 1d, which employs a cascade of two nonlinear resonators (one Lorentzian and one Fano). But nevertheless, this limitation, as well as the distortion induced by nonlinearity, precludes the use of such non-reciprocal components in most electronic applications where linearity is critical. Nonlinear isolators are also limited by a dynamic reciprocity mechanism[36] — in the presence of a strong incident signal, the response to a second weak signal is reciprocal across the two ports. In general, nonlinear isolators operate well when excited from a single port, and their functionality becomes complicated when excited at both ports simultaneously[37].

Non-reciprocity based on temporal modulation of permittivity

In the 1950s, parametric amplifiers or variable reactance amplifiers emerged as an alternative to vacuum-tube amplifiers for low-noise amplification applications[38]. In these amplifiers, typically the capacitance of a semiconductor diode was modulated with a pump signal to impart gain to the desired signal. These amplifiers took two forms — upconversion-type or negative-resistance/reflection-type parametric amplifiers. In the former, the gain was accompanied by an upconversion of the signal to a frequency equal to the sum of the input frequency and the pump frequency. The latter were one-port devices where the pump signal was at twice the input frequency, imparting gain at the input frequency and thereby realizing a negative resistance or a reflection of the incident wave with gain. These latter devices required circulators to separate the incoming and amplified outgoing waves, thus prompting a research effort into the realization of non-reciprocal circulation and isolation using non-magnetic parametric techniques[39–41]. In ref. [39], the author exploits the frequency-conversion characteristics of two semiconductor-diode parametric circuits with phase-shifted pump

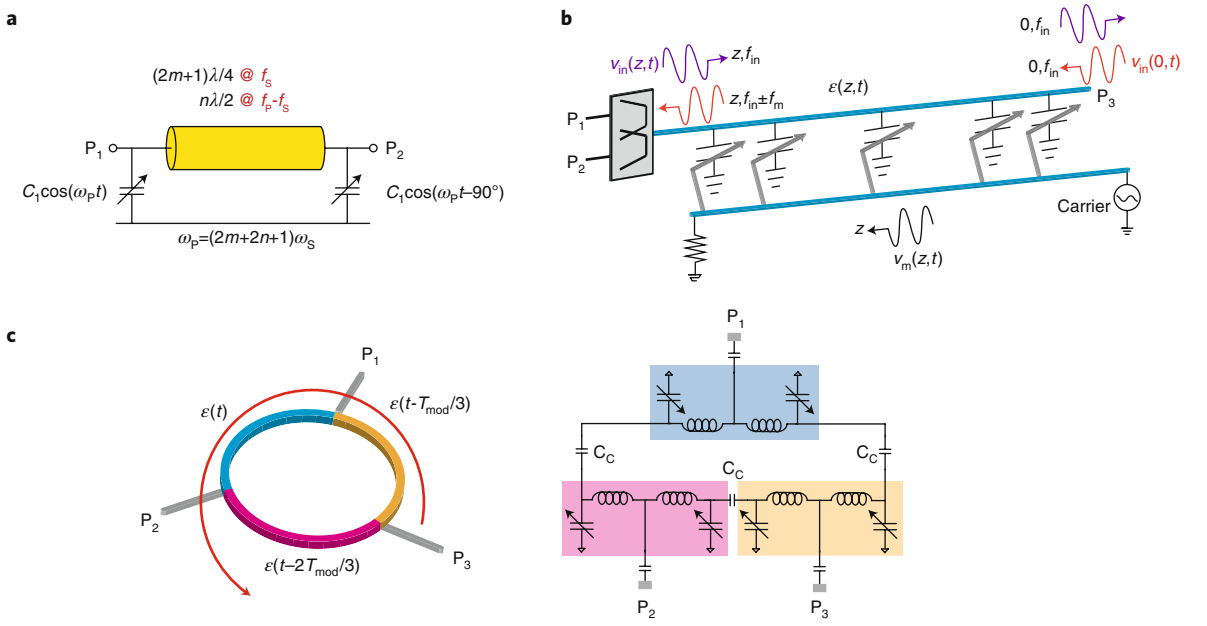

Fig. 2 | Non-reciprocity based on temporal modulation of permittivity or capacitance. a, Parametric non-reciprocal device based on temporal modulation of semiconductor-diode capacitances across a transmission-line delay with a modulation frequency ω_P[39]. $C_1\cos(\omega_P t)$ and $C_1\cos(\omega_P t-90°)$ represent the capacitance profile of the diode capacitors on the left and the right. C_1, modulation amplitude; t, time; f_S, signal frequency; f_P, pump frequency; λ, wavelength. **b**, Non-reciprocal wave propagation accompanied by frequency conversion through traveling-wave modulation of capacitance along a transmission line where f_{in} and f_m represent the input and modulation frequencies, and v_{in} and v_m represent the input and modulation travelling waves, respectively.[47]. **c**, Angular momentum biasing in coupled resonant rings using coupling capacitors C_C to realize circulation without frequency conversion at the ports[50]. T_{mod}, modulation time period.

signals and separated by a quarter-wave transmission line to realize passive temporally modulated gyrators and circulators (Fig. 2a). This architecture is a precursor to the approaches being pursued recently in the microwave and photonic domains.

While parametric amplifiers and non-reciprocal components took a back seat in the following years due to the ascent of semiconductor transistors and integrated circuits, similar approaches based on electro-optic refractive-index modulation have been explored in the optical domain. In refs. [42,43], a pair of electro-optic phase modulators separated by an optical delay is used to obtain isolation. An alternative approach is traveling-wave refractive-index modulation along a waveguide, which produces a direction-dependent frequency conversion for the desired signal within the waveguide[44–46]. The traveling-wave approach has more recently been investigated in the microwave domain through modulation of varactor diodes along a transmission line[47]. The direction-dependent frequency conversion of the desired signal allows signals traveling in opposite directions to be separated using a duplexer filter (Fig. 2b). Aside from the trade-offs associated with permittivity or capacitance modulation, which will be discussed shortly, the translation of signals traveling in one direction to another frequency is undesirable in some applications. This can be avoided through the biasing of angular momentum through traveling-wave modulation in resonant rings. Explored extensively in the acoustic domain through the mechanical spinning of a fluid[48], at optical frequencies through traveling-wave modulation in ring resonators[49], as well as at microwave frequencies in coupled-resonator loops[50,51], this approach avoids frequency conversion at the ports (Fig. 2c).

All of these approaches fundamentally fall within the category of spatio-temporal permittivity/refractive-index/capacitance modulation, where permittivity/refractive index/capacitance are modulated in time and space (that is, the modulation signal is applied at different points in space and with time or phase shifts). A fundamental trade-off with spatio-temporal modulation of any kind is between modulation depth and size. If the modulated parameter (in these cases, permittivity or refractive index or capacitance) can be varied only over a limited range, then the modulation needs to be performed over a larger spatial dimension to achieve strong non-reciprocity. Resonances can be used to miniaturize the size, but the bandwidth of the structure would correspondingly reduce. There also exists a trade-off between modulation frequency, size, and bandwidth — modulation at lower frequencies is desirable to reduce the complexity of the modulation circuitry, but the size of the structure must correspondingly increase and the bandwidth of the structure correspondingly reduces.

A fundamental challenge with permittivity modulation is the limited range over which it can be modulated. At optical frequencies, the modulation index $(\triangle\varepsilon/\varepsilon)$ of the permittivity of the medium (ε) is typically fractions of a percent, resulting in non-reciprocal components that are often thousands of wavelengths in size. At radio and microwave frequencies, varactors on a semiconductor substrate typically achieve modulation ratios (C_{max}/C_{min}, where C_{max} and C_{min} are, respectively, the maximum and minimum capacitances achieved by the varactor) of 2–4, which is appreciable compared to optical materials but still limits the size-bandwidth trade-off. Therefore, while varactor modulation approaches, specifically those based on angular momentum biasing, have been able to achieve insertion losses of around 2 dB and near watt-level power handling when implemented using discrete components on a printed circuit board (PCB)[51], the bandwidth tends to be limited to ~2% of the operating frequency as the price for miniaturization of the size to sub-wavelength dimensions and the use of a modulation frequency that is, for instance, one-tenth of the operating frequency (100 MHz for 1 GHz operation in ref. [51]). First efforts towards integrated-circuit implementations of varactor-modulation approaches have emerged[52], and one may expect enhancements in performance through further research.

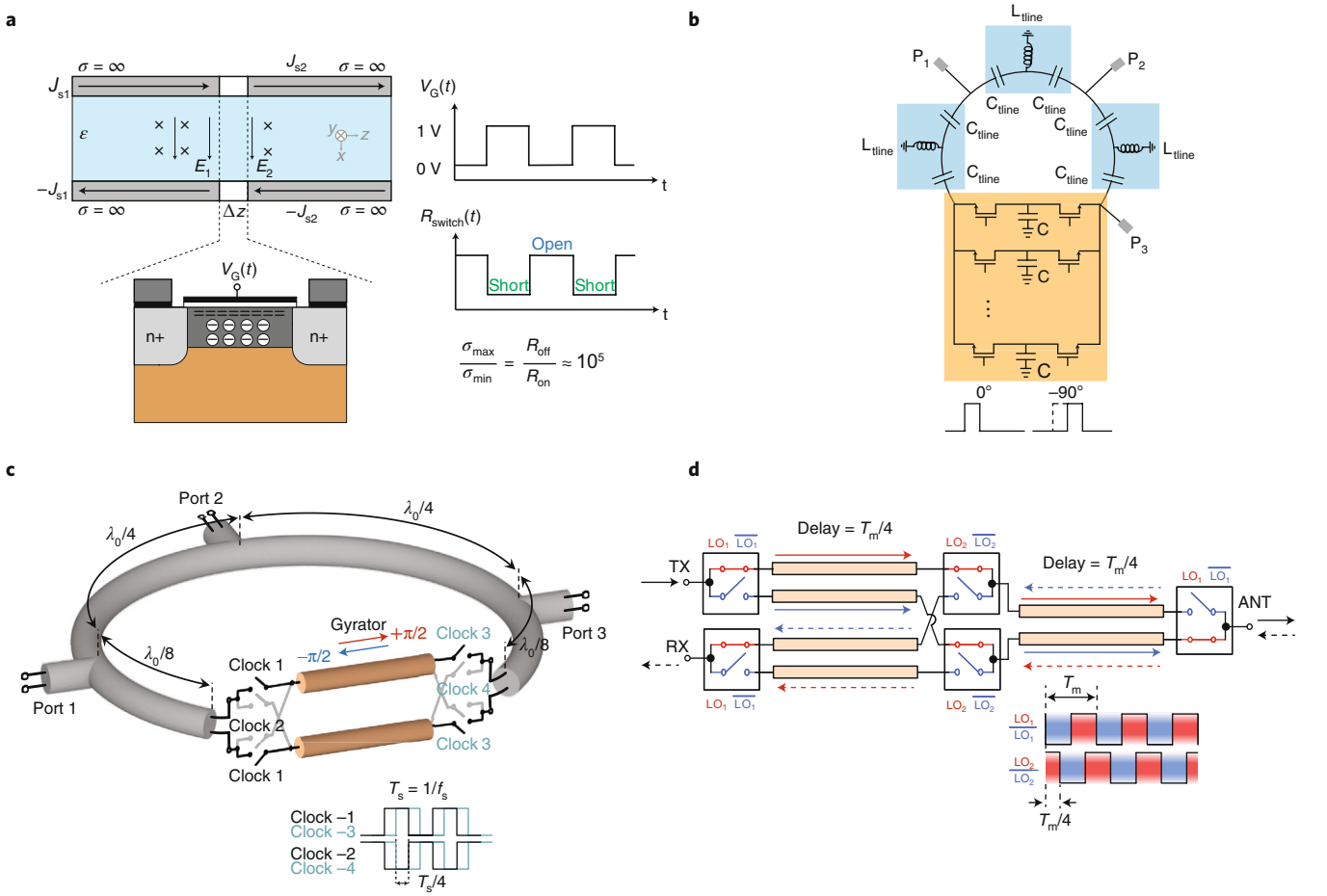

Fig. 3 | Non-reciprocity through temporal conductivity modulation on semiconductor substrates. a, Embedding dynamically-modulated passive reciprocal transistor switches within electromagnetic structures to realize high-contrast conductivity modulation using the ON (σ_{min}) and OFF (σ_{max}) states of the transistor switches. J_{s1} and J_{s2}, sheet resistance of the signal and ground conductors, respectively; E_1 and E_2, electric fields in the semiconductors on the left and right, respectively; σ, conductivity; V_G, gate voltage; R_{switch}, transistor switch resistance; R_{off} and R_{on}, resistances of the switch in the OFF and ON states, respectively. **b**, CMOS circulator based on an *N*-path filter gyrator[24], employing staggered commutation around a bank of capacitors *C* combined with a $3\lambda/4$ transmission line implemented using lumped inductors L_{line} and capacitors C_{line}. **c**, CMOS circulator based on a switched transmission-line gyrator, employing staggered commutation around delay lines with a modulation frequency of f_s and combined with $3\lambda/4$ transmission line[21], enabling watt-level power handling at RF[20] and millimetre-wave operation[21]. **d**, An ultra-wideband circulator based on sequentially-switched delay lines with a modulation period of T_m[23]. TX, transmitter; ANT, antenna; RX, receiver. $LO_{1,2}$ are the clock waveforms provided to the various switches.

Non-reciprocity based on temporal modulation of conductivity

On the other hand, semiconductors are fundamentally amenable to strong conductivity modulation — the conductance of a passive transistor switch in a modern CMOS process can be varied by a factor of 10^3–10^5 (ref. [53]). As a result, there has been a growing body of work investigating integrated-circuit non-reciprocal components exploiting switch-based conductivity modulation (Fig. 3).

Achieving non-reciprocity though dynamic switching dates back to 1960s[54], where synchronized switching around transmission-line delays enabled multi-port circulation and isolation. Recently, it has been shown that staggered switching in commutated networks breaks time reversal symmetry and enables phase non-reciprocity in extremely compact dimensions[24]. In this work, two sets of commutating switches on either side of a bank of capacitors was considered, a circuit commonly called the *N*-path filter (Fig. 3b)[55]. The *N*-path filter circuit dates back to the 1940s and 1950s, with first implementations relying on mechanical commutation through a rotating brush that periodically contacted a bank of capacitors[56,57] to realize narrow comb filters around harmonics of the commutation frequency. More recently, electronic commutation using passive transistor-based switches has resulted in high quality-factor (*Q*) comb filters which operate at radio frequency (RF) without the need for inductors[55], exhibit substantially lower noise and higher linearity when compared with active RF filters, and are compatible with conventional CMOS integrated circuit (IC) fabrication. In ref. [24], it was shown that staggering the clocks of the switches on either side of the capacitor bank enables phase non-reciprocity and the realization of an extremely-compact (effectively infinitesimal) non-magnetic gyrator, which was then used to realize the first CMOS passive non-magnetic circulator (Fig. 3b). In this work, and in *N*-path filters in general, the clock frequency is the same as the operating frequency (750 MHz; ref. [24]), and multiple phases are required for commutation (typically 4 or 8).

Later, inspired from this work, generalized switched transmission-line structures were proposed to realize wideband and/or high-frequency non-reciprocity[20–23]. These structures exploit delay lines, instead of capacitors, between the commutated switches to realize extremely wideband non-reciprocal responses (Fig. 3c). The wideband response of a gyrator realized in such a fashion implies larger bandwidth of the resultant circulator. Additionally, it decouples the signal frequency f_{in} from the modulation frequency

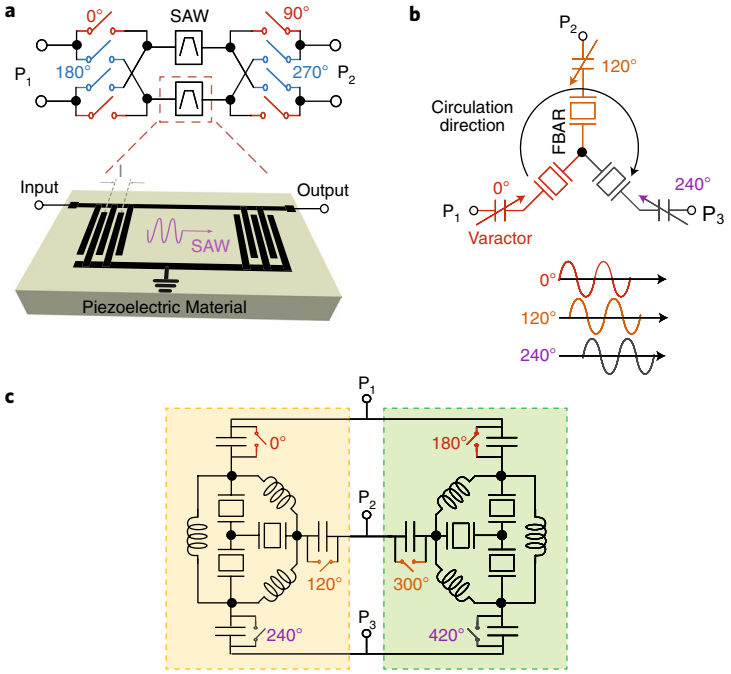

Fig. 4 | Non-reciprocity in hybrid electro-acoustic devices. a, Switched-SAW-filter gyrator[64], where the SAW filter replaces the transmission lines in the switched-transmission-line gyrator of refs. [21,22]. **b**, FBAR circulator based on angular momentum biasing through the modulation of the series resonance frequency of FBARs using varactors[60]. **c**, Angular momentum biased circulator based on switch-based commutation of FBAR resonators[61]. All these works exploit the high *Q* and time delays achievable in acoustics to lower modulation frequency and associated power consumption.

f_m, allowing the lowering of the modulation frequency with a constraint of appropriately increasing the length of the transmission lines between the switches. This feature has been leveraged to implement high-performance CMOS circulators (Fig. 3c) with watt-class power handling at radio frequencies[20], and millimetre-wave CMOS circulators at 25 GHz (ref. [21]; 8.33 GHz modulation frequency) and 60GHz (ref. [58]; 8.6 GHz modulation frequency). Similar structures have also been used to implement the first extremely wideband circulators operating from d.c. to RF frequencies (Fig. 3d)[23,59]. For lossless operation in the switched-transmission-line gyrator, the transmission lines between the switches must be able to support all intermodulation frequencies created by mixing the input and the modulation signal. Distributed transmission lines that can provide the required delay for lower modulation frequencies occupy a large area in CMOS ICs. Quasi-distributed implementations using lumped-inductor–capacitor (LC) sections can further miniaturize the device size as shown in refs. [20,21,58]. Such implementations need to include enough LC sections to provide a sufficiently large cut-off frequency, also known as Bragg frequency. Quasi-distributed transmission lines can potentially be used in the previously discussed parametric permittivity-modulation-based implementations such as the one described in ref. [47]. The number of lumped stages in such devices should be decided based on the varactor's modulation ratio and the required modulation strength.

The enhanced linearity of passive-transistor-switch circuits over active-transistor-based circuits arises from the fact that passive transistor-based switches are typically modulated with square-wave signals that hard-switch between the ground and supply rails. Consequently, the input signal levels that become comparable to the supply voltage and produce nonlinearity are higher than those that become comparable to the bias levels of active-transistor-based circuits, which are typically biased well below the supply voltage. Moreover, in a well-designed switching circuit, the parasitic switch resistance is substantially lower than the impedance levels of the circuit in order to minimize loss. Therefore, nonlinearity in the switch resistance has a reduced impact on the response of the circuit as a whole. The noise advantage of passive-transistor-switch circuits over active circuits is the fact that the thermal noise of transistor switch is equal to that of a resistor with the same ON resistance, which is typically made small relative to the circuit impedance, as mentioned earlier. Active transistors typically exhibit excess noise as a direct consequence of their active biasing. The drawback of a passive transistor switch is that it is unable to impart power gain, unlike an active transistor. However, gain is not a requirement for non-reciprocal components such as circulators and isolators. In fact, in other classes of circuits beyond non-reciprocity, such as frequency-conversion mixers, passive-switch-based mixers have almost completely replaced active-transistor mixers when gain is not required.

When contrasting conductivity modulation with permittivity modulation, we note that the limited modulation contrast of permittivity results in large sizes in non-resonant approaches, such as the traveling-wave approach in ref. [47], and the need for higher-*Q* resonators in resonant approaches such as angular momentum biasing, compromising the bandwidth. While conductivity modulation addresses the issue of contrast, we note that transistor switches must be hard switched between the supply and the ground rails, so that they go from an infinite-resistance state to a near-zero-resistance state. Intermediary states of finite resistance will produce loss. The need for multiple phases of such hard-switching square-wave clocks limits the highest modulation frequency that can be supported by a semiconductor technology, which in turn will limit the highest frequency at which such non-reciprocal components can be implemented. Furthermore, multi-phase square-wave clocks driving passive transistor switch circuits are most easily implemented in integrated-circuit technology, but would be challenging in discrete electronics settings, where the simplicity of sine-wave-modulated varactors eases the implementation of permittivity-modulated non-reciprocal components. Finally, since permittivity is an energy-storage parameter, its modulation can yield parametric gain, which is physically impossible with conductivity modulation.

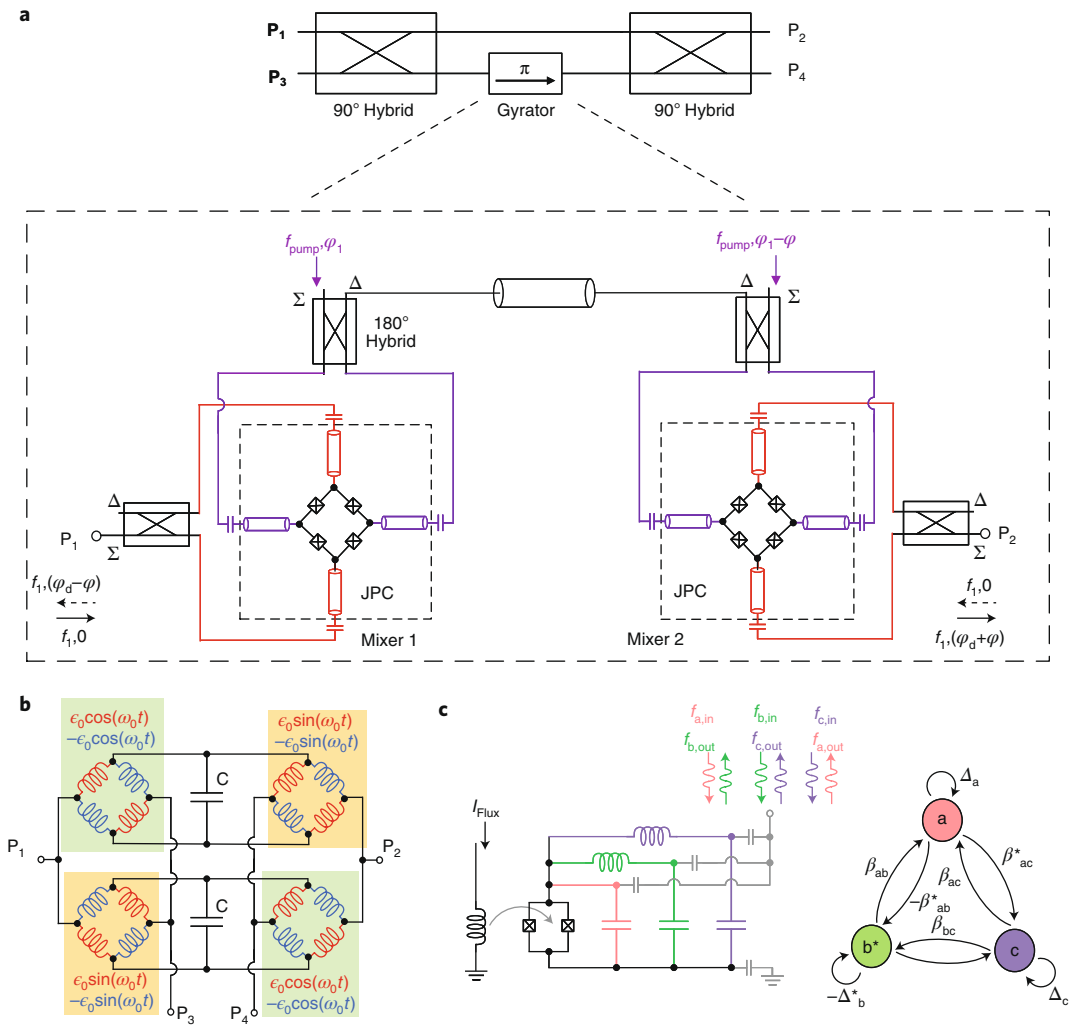

Fig. 5 | Non-reciprocity through time-variance at cryogenic temperatures targeting quantum computing applications. a, A four-port circulator can be built by integrating a gyrator into a Mach–Zehnder interferometer. The gyrator is implemented using the mixer-delay-mixer architecture where two Josephson parametric converters (JPCs) are used as frequency-conversion mixers[69]. The mixers in the gyrator are modulated using two pump tones with a frequency of f_{pump} and a relative phase-shift of φ to imprint the non-reciprocal phase shift on the transmitted signal. φ_d is the phase shift provided by the delay line between the two pump signals. Δ and Σ are the difference and summing ports of the hybrid coupler, respectively. **b**, Lumped-element schematic of a widely tunable microwave on-chip circulator[17] built using dynamically modulated d.c. superconducting quantum interference devices (SQUIDs) through flux lines (not shown). Inductances in the bridge circuits are tuned dynamically as $L/(1 \pm \epsilon_0\cos(\omega_0 t))$ and $L/(1 \pm \epsilon_0\sin(\omega_0 t))$, where L is the nominal inductance of the squid device, $\epsilon_0\cos(\omega_0 t)$ and $\epsilon_0\sin(\omega_0 t)$ represent the modulation profiles of the inductances, ϵ_0 is the amplitude of the tuning, ω_0 is the angular modulation frequency. **c**, A superconducting reconfigurable non-reciprocal microwave signal processor exploiting non-reciprocity in frequency-space, with three resonances f_a, f_b and f_c whose frequencies are tunable by the flux applied to a single SQUID, and a graphical representation of the equation of motion of the three-resonant circuit where Δ_j (j = a,b,c) represent the normalized detuning for mode j and β_{jk} (j,k = a,b,c) represent the normalized couple of the modes j and k (ref. [71]). $f_{j,in}$ and $f_{j,out}$ represent the input and output waves at frequencies f_j.

Non-reciprocal hybrid acoustic–electronic components

Lower modulation frequency is typically preferred due to the associated lower complexity in the modulation circuitry, lower power consumption, and lower switching losses. Excessive lowering of the modulation frequency in the switched delay-line structures results in very long delay lines, and consequently larger footprints and associated losses. On the other hand, acoustic-wave (surface acoustic-wave, SAW; and film bulk acoustic resonator, FBAR) devices and microelectromechanical systems (MEMS) resonators provide large group delays and higher-quality resonators within a smaller footprint when compared with on-chip electromagnetic passive structures due to the low acoustic wave velocity. This has led to a growing body of work exploring hybrid acoustic–electronic non-reciprocal components. These efforts include approaches employing angular momentum biasing in FBAR devices and MEMS resonators, with steadily improving performance metrics[60–63], as well as circulators that replace the switched-transmission line gyrator with a switched-SAW gyrator[64]. Fig. 4a depicts the switched-SAW gyrator of ref. [64], while Fig. 4b depicts an FBAR circulator based on angular momentum biasing achieved through modulation of the series resonance frequency of FBAR resonators using varactors[60]. Fig. 4c depicts an FBAR circulator that also exploits angular momentum biasing, but achieved through switch-based commutation to achieve high performance[61].

Non-reciprocal components for quantum computing applications

Circulators and isolators also play a prominent role in the readout of qubits in superconducting quantum computing applications[65].

The state of a superconducting qubit operating at cryogenic temperatures ranging between 10–100 mK is read out by measuring the state dependent phase shift imparted to a probe signal. A substantial amplification is required for the readout signal before it reaches the room temperature circuitry, and is typically achieved through multiple stages of amplification. The first stage of amplification is typically realized within the cryogenic chamber (that is, dilution refrigerator) using Josephson parametric amplifiers (JPAs) to amplify the signal with very little added noise (near quantum limits)[66]. These JPAs are implemented using the nonlinear inductance of Josephson Junctions (JJs)[67,68]. JPAs are implemented as single-port reflection amplifiers emulating a negative resistance, and therefore, a circulator is crucial for their operation to separate the input signal from the amplified reflected signal. The second stage of amplification is performed using a cryogenic, high-electron-mobility transistor (HEMT) amplifier which sits at a higher temperature of 3–4 K. The noise generated at the input of the HEMT acts as a hot blackbody noise source which could potentially corrupt the state of the quantum circuits. To avoid this, the JPAs are typically followed by a set of circulators and isolators to protect the quantum circuits from this noise. In these applications as well, ferrite circulators are currently widely used. However, the bulky form factor of the ferrite circulator occupies substantial space in the dilution refrigerator, limiting the maximum number of qubits that can be operated simultaneously[65]. Recognition of the need for a low cost, compact and scalable circulator has therefore motivated the investigation of alternate means for generating non-reciprocity, with some of the initial approaches including parametric JJ circulators, multimode parametric devices, and circulators with synthetic rotation.

The nonlinearity of the JJ is commonly leveraged to create parametric interaction between the signal and pump tones, and consequently a low-loss frequency mixing. In ref. [69], gyrator operation has been demonstrated by connecting two three-wave mixer stages through a transmission line (Fig. 5a). This architecture is closely related to the switched transmission-line architecture discussed earlier, with the frequency-conversion mixers realized using Josephson parametric converters (JPCs)[70]. This gyrator could then be incorporated within a Mach–Zehnder interferometer employing two 90° hybrids to realize a multi-port circulator (Fig. 5a). In ref. [17], it has been shown that a differential gyrator realized using the mixer–delay–mixer configuration can also act as a 4-port circulator when excited using 4 individual ports (Fig. 5b), hence, omitting the 90° microwave hybrids required for circulation and enabling a circulator with extremely compact footprint.

The aforementioned circulators feature input and output signals at the same frequency despite the internal frequency conversion. Some efforts have been devoted to create non-reciprocity in the frequency space (between various different frequencies as shown in Fig. 5c) instead of spatial modes at the same frequency[71,72]. For instance, ref. [71] describes a field-programmable Josephson amplifier capable of reconfigurable non-reciprocal microwave signal processing. The field programmability, achieved through different configurations of pump signals, enables different operation configurations — low-loss frequency conversion between frequency modes, bidirectional amplification between frequency modes, non-reciprocal circulation between frequency modes, and non-reciprocal amplification between frequency modes.

Outlook

Research on non-magnetic non-reciprocal electronic devices has recently spread across various platforms, from CMOS to acoustic-wave devices to cryogenic superconducting circuits, with the best implementations reaching sub-3-dB insertion loss levels and watt-level power handling. The critical bottleneck for further improvement in transmission losses, particularly for CMOS IC implementations, is the poor quality of on-chip passive components. Co-integration of chip-scale non-reciprocal components with high-quality passive components, either above the IC or within the package, represents a promising route to improving insertion loss levels while maintaining a compact footprint.

Power handling is limited by the breakdown voltage of the transistor technology used. To further improve power handling, series device stacking techniques in the time-modulated transistors to share the voltage stress across multiple devices could be explored[73,74]. However, this comes at the expense of other switch performance metrics such as the ON resistance and the maximum switching frequency. Also, these techniques do not overcome the fundamental trade-off between the power handling of a switch and the power consumption required to modulate it, which is limited by the switch technology used. On the other hand, III–V/III–N compound semiconductor technologies (such as GaAs and GaN) exhibit superior Johnson Limit (speed-breakdown voltage trade-off) to CMOS, and also integrate high-quality passives due to the insulating nature of the substrate and the use of gold metallization, but lack the high transistor density and yield offered by CMOS. Hence, heterogeneous integration of GaAs/GaN with CMOS, whereby the signal path comprising the switches and the passive components are integrated in GaAs/GaN, and CMOS technology is used for the generation of the complex modulation signals, represents a promising direction[75].

Along with the reduced size, weight, and implementation cost, integrated non-reciprocal components offer an exciting opportunity for co-design with the rest of the electronic system. In one such early effort[19], a CMOS circulator–receiver architecture was demonstrated based on the insight that each set of switches in the *N*-path filter implements a mixer, thus enabling the baseband voltages to be directly accessible across the *N*-path capacitors and eliminating the need for the low-noise amplifier and down-conversion mixer required in traditional receivers. This concept has been further scaled to array implementations for full-duplex multi-antenna systems, including phased-array circulator–receiver arrays[76] and multi-input multi-output (MIMO) arrays[77]. The integration of antenna tuners and self-interference leakage cancellers within CMOS circulators has also been demonstrated[19,20,76,77], enabling these circulators to have high-isolation despite antenna impedance variations.

Non-reciprocal antennas that may transmit/receive but not receive/transmit, or do so from different ports, or transmit and receive with different beam patterns also represent an interesting research direction. Initial explorations include temporal modulation in graphene[78], traveling-wave antennas[79] and leaky-wave antennas[80]. In particular, in ref. [80], a time-modulated leaky-wave antenna system effectively merging an antenna, a circulator, and a mixer was proposed, allowing the device to operate as a complete transceiver. Recently, commutated switched-capacitor circuits have been shown to overcome the delay-bandwidth limit through quasi-electrostatic wave propagation[81], enabling wideband reciprocal and non-reciprocal delays within an extremely small footprint, potentially opening the door to new classes of fully-integrated, compact, and widely-reconfigurable reciprocal and non-reciprocal microwave components.

Although time modulated circuits have been studied for more than five decades, their formal theoretical analysis remains challenging, and numerical methods with large computational requirements are often used to model their operation. This problem arises because time modulation leads to frequency translation of the signals to inter-modulation frequencies, and so traditional linear time-invariant (LTI) circuit analysis techniques such as the Laplace transform and the Fourier transform have limited applicability. The behaviour of time-modulated devices with small modulation contrasts, such as nonreciprocal devices based on permittivity modulation[47,82,83], is modelled using coupled mode analysis and techniques of perturbation theory. However, for large modulation contrasts, such as those achieved with conductivity modulation, these approaches lead to inaccurate solutions as they model only the first-order intermodulation product.

A more accurate analysis technique for hard-switching circuits has been developed[84] based on time-domain polyphase kernels. The approach was also applied to the *N*-path filter gyrator[85]. While this technique provides a closed form expression for the circuit operation, the construction of these kernels and calculation of the corresponding boundary conditions becomes challenging with an increase in the circuit complexity. Recently, frequency-domain circuit analysis techniques based on conversion matrices[86] and Floquet scattering matrices (FSM)[22] have been introduced for numerically computing the solutions of time-modulated circuits and systems. Since their framework fundamentally uses matrices, they are more structured, readily scalable, and easier to implement on modern-day processors using commercially available programming software. In another effort targeting sampled systems, a simplified analysis of harmonic transfer functions (HTF) was proposed by using adjoint networks[87]. More recently, a new method was proposed by decomposing the linear periodically time varying (LPTV) networks into a finite number of LTI networks and accurately describing their behaviour with semi-analytical equations[88]. This method is enabled by modelling the time-modulated devices using a set of controlled sources in parallel with a resistor. Despite these recent efforts, a more generalized theoretical framework that yields closed-form expressions and intuition is critical for a better understanding of the operation of generalized time-modulated systems, and to aid in the discovery of new architectures.

Inspired by the exciting discoveries of condensed matter systems exhibiting topological order[89,90], there has been substantial recent interest in demonstrating analogous systems for classical waves through the engineering of topological order within acoustic[91,92] and photonic/electromagnetic metamaterials. However, to date, demonstrations of photonic and electromagnetic topological metamaterials with non-reciprocal responses have relied on magneto-optic effects[93–95]. Integrated-circuit temporally modulated non-reciprocal components, such as the ones discussed in this Review Article, can serve as an ideal building block for the realization of Floquet electromagnetic topological metamaterials due to the robustness and repeatability of IC fabrication processes. Such topological metamaterials will not only offer new opportunities to probe the exciting physics of topological order, but may also find application as highly reconfigurable, robust, non-reciprocal signal routing fabrics.

Received: 27 October 2019; Accepted: 20 March 2020;
Published online: 4 May 2020

References

1. Cannell, D. M. *George Green: Mathematician and Physicist 1793–1841: The background to his life and work*. 2nd edn, 190–192 (Society for Industrial and Applied Mathematics, 2001).
2. Rayleigh, J. W. S. B. *Theory of Sound*. 1st edn, Vol. 1 Ch. V. (Macmillan and Co., 1896).
3. Helmholtz, H. On the physical significance of the principle of least action. *J. Reine Angew. Math.* **100**, 217–222 (1886).
4. Lorentz, H. A. Het theorema van Poynting over de energie in het electromagnetisch veld en een paar algemeene stellingen over de voortplanting van het licht. *In Verslagen der Afdeeling Natuurkunde van de Koninklijke Akademie van Wetenschappen* **4**, 176–187 (1895).
5. Carson, J. R. Reciprocal theorems in radio communication. *Proc. IRE* **17**, 952–956 (1929).
6. Ballantine, S. Reciprocity in electromagnetic, mechanical, acoustical, and interconnected systems. *Proc. IRE* **17**, 927–951 (1929).
7. Onsager, L. Reciprocal relations in irreversible processes. *I. Phys. Rev* **37**, 405–426 (1931).
8. Casimir, H. B. G. On Onsager's principle of microscopic reversibility. *Rev. Mod. Phys.* **17**, 343–350 (1945).
9. De Hoop, A. T. A reciprocity relation between the transmitting and the receiving properties of an antenna. *App. Sci. Res* **19**, 90–96 (1968).
10. Jalas, D. et al. What is — and what is not — an optical isolator. *Nat. Photon* **7**, 579–582 (2013).
11. Fan, S. et al. Comment on 'Nonreciprocal light propagation in a silicon photonic circuit'. *Science* **335**, 38–38 (2012).
12. Tellegen, D. The gyrator, a new electric network element. *Philips Res. Rep* **3**, 81–101 (1948).
13. Hogan, C. L. The ferromagnetic Faraday effect at microwave frequencies and its applications: the microwave gyrator. *Bell Syst. Tech. J* **31**, 1–31 (1952).
14. Gardner, D. S. et al. Review of on-chip inductor structures with magnetic films. *IEEE Trans. Magn.* **45**, 4760–4766 (2009).
15. Zhou, J. et al. Integrated full duplex radios. *IEEE Commun. Mag.* **55**, 142–151 (2017).
16. van Liempd, B. et al. A +70-dBm IIP3 electrical-balance duplexer for highly integrated tunable front-ends. *IEEE Trans. Microw. Theory Techn* **64**, 4274–4286 (2016).
17. Chapman, B. J. et al. Widely tunable on-chip microwave circulator for superconducting quantum circuits. *Phy. Rev. X* **7**, 041043 (2017).
18. JQL Electronics. Accessed on: 2020. [Online]. Available: http://www.jqlelectronics.com/
19. Reiskarimian, N., Baraani Dastjerdi, M., Zhou, J. & Krishnaswamy, H. Analysis and design of commutation-based circulator-receivers for integrated full-duplex wireless. *IEEE J. Solid State Circ* **53**, 2190–2201 (2018).
20. Nagulu, A. & Krishnaswamy, H. Non-magnetic CMOS switched-transmission-line circulators with high power handling and antenna balancing: theory and implementation. *IEEE J. Solid State Circ* **54**, 1288–1303 (2019).
21. Dinc, T. et al. Synchronized conductivity modulation to realize broadband lossless magnetic-free non-reciprocity. *Nat. Commun.* **8**, 795 (2017).
22. Nagulu, A. et al. Nonreciprocal components based on switched transmission lines. *IEEE Trans. Microw. Theory Techn* **66**, 4706–4725 (2018).
23. Biedka, M. M., Zhu, R., Xu, Q. M. & Wang, Y. E. Ultra-wide band non-reciprocity through sequentially-switched delay lines. *Sci. Rep* **7**, 40014 (2017).
24. Reiskarimian, N. & Krishnaswamy, H. Magnetic-free non-reciprocity based on staggered commutation. *Nat. Commun.* **7**, 11217 (2016).
25. Tanaka, S., Shimomura, N. & Ohtake, K. Active circulators–the realization of circulators using transistors. *Proc. IEEE* **53**, 260–267 (1965).
26. Mung, S. W. & Chan, W. S. The challenge of active circulators: design and optimization in future wireless communication. *IEEE Microw. Mag.* **20**, 55–66 (2019).
27. Kodera, T., Sounas, D. L. & Caloz, C. Magnetless nonreciprocal metamaterial (MNM). *technology: application to microwave components. IEEE Trans. Microw. Theory Techn* **61**, 1030–1042 (2013).
28. Carchon, G. & Nanwelaers, B. Power and noise limitations of active circulators. *IEEE Trans. Microw. Theory Techn* **48**, 316–319 (2000).
29. Peng, B. et al. Parity-time-symmetric whispering-gallery microcavities. *Nat. Phys* **10**, 394–398 (2014).
30. Fan, L. et al. An all-silicon passive optical diode. *Science* **335**, 447–450 (2012).
31. Nazari, F. et al. Optical isolation via PT-symmetric nonlinear Fano resonances. *Opt. Express* **22**, 9574–9584 (2014).
32. Mahmoud, A. M., Arthur, R. D. & Engheta, N. All-passive nonreciprocal metastructure. *Nat. Commun.* **6**, 8359 (2015).
33. Sounas, D. L., Soric, J. & Alù, A. Broadband passive isolators based on coupled nonlinear resonances. *Nat. Elec* **1**, 113 (2018).
34. D'Aguanno, G., Sounas, D. L. & Alù, A. Nonlinearity-based circulator. *Appl. Phys. Lett.* **114**, 181102 (2019).
35. Hadad, Y., Soric, J. C., Khanikaev, A. B. & Alù, A. Self-induced topological protection in nonlinear circuit arrays. *Nat. Elec* **1**, 178–182 (2018).
36. Shi, Y., Yu, Z. & Fan, S. Limitations of nonlinear optical isolators due to dynamic reciprocity. *Nat. Photon* **9**, 388–392 (2015).
37. Sounas, D. L. & Alù, A. Nonreciprocity Based on Nonlinear Resonances. *IEEE Antenn. Propag. Lett* **17**, 1958–1962 (2018).
38. Reed, E. D. The variable-capacitance parametric amplifier. *IRE Trans. Electron. Devices* **6**, 216–224 (1959).
39. Kamal, A. A parametric device as a nonreciprocal element. *Proc. IRE* **48**, 1424–1430 (1960).
40. Baldwin, L. Nonreciprocal parametric amplifier circuits. *Proc. IRE* **49**, 1075 (1961).
41. Hamasaki, J. A theory of a unilateral parametric amplifier using two diodes. *Bell Syst. Tech. J* **43**, 1123–1147 (1964).
42. Galland, C., Ding, R., Harris, N. C., Baehr-Jones, T. & Hochberg, M. Broadband on-chip optical non-reciprocity using phase modulators. *Opt. Express* **21**, 14500–14511 (2013).
43. Doerr, C. R., Chen, L. & Vermeulen, D. Silicon photonics broadband modulation-based isolator. *Opt. Express* **22**, 4493–4498 (2014).
44. Lira, H., Yu, Z., Fan, S. & Lipson, M. Electrically driven nonreciprocity induced by interband photonic transition on a silicon chip. *Phys. Rev. Lett.* **109**, 033901 (2012).
45. Kang, M., Butsch, A. & Russell, P. S. J. Reconfigurable light-driven opto-acoustic isolators in photonic crystal fibre. *Nat. Photon* **5**, 549–553 (2011).
46. Yu, Z. & Fan, S. Complete optical isolation created by indirect interband photonic transitions. *Nat. Photon* **3**, 91–94 (2008).

47. Qin, S., Xu, Q. & Wang, Y. Nonreciprocal components with distributedly modulated capacitors. *IEEE Trans. Microw. Theory Techn* **62**, 2260–2272 (2014).
48. Fleury, R., Sounas, D. L., Sieck, C. F., Haberman, M. R. & Alù, A. Sound isolation and giant linear nonreciprocity in a compact acoustic circulator. *Science* **343**, 516–519 (2014).
49. Sounas, D. L. & Alù, A. Angular-momentum-biased nanorings to realize magnetic-free integrated optical isolation. *ACS Photon* **1**, 198–204 (2014).
50. Estep, N. A., Sounas, D. L., Soric, J. & Alù, A. Magnetic-free non-reciprocity and isolation based on parametrically modulated coupled-resonator loops. *Nat. Phys* **10**, 923–927 (2014).
51. Kord, A., Sounas, D. L. & Alù, A. Pseudo-linear time-invariant magnetless circulators based on differential spatiotemporal modulation of resonant junctions. *IEEE Trans. Microw. Theory Tech* **66**, 2731–2745 (2018).
52. Kord, A., Tymchenko, M., Sounas, D. L., Krishnaswamy, H. & Alù, A. CMOS integrated magnetless circulators based on spatiotemporal modulation angular-momentum biasing. *IEEE Trans. Microw. Theory Tech* **67**, 2649–2662 (2019).
53. Tyagi, S. et al. An advanced low power, high performance, strained channel 65nm technology. In *2005 IEEE Int. Electron Devices Meet. Tech. Digest* 245–247 (IEEE, 2005).
54. Mohr, R. J. A new nonreciprocal transmission line device. *Proc. IEEE* **52**, 612 (1964).
55. Ghaffari, A., Klumperink, E. A. M., Soer, M. C. M. & Nauta, B. Tunable high-*Q N*-path band-pass filters: modeling and verification. *IEEE J. Solid State Circ* **46**, 998–1010 (2011).
56. Busignies, H. & Dishal, M. Some relations between speed of indication, bandwidth, and signal-to-random-noise ratio in radio navigation and direction finding. *Proc. IRE* **37**, 478–488 (1949).
57. LePage, W. R., Cahn, C. R. & Brown, J. S. Analysis of a comb filter using synchronously commutated capacitors. *Trans. Am. Inst. Electric. Eng. I* **72**, 63–68 (1953).
58. Nagulu, A. & Krishnaswamy, H. Non-magnetic 60GHz SOI CMOS circulator based on loss/dispersion-engineered switched bandpass filters. In 2019 IEEE Int. Solid State Circuits Conf. (ISSCC) 446–448 (IEEE, 2019).
59. Lu, R., Krol, J., Gao, L. & Gong, S. Frequency independent framework for synthesis of programmable non-reciprocal networks. *Sci. Rep* **8**, 14655 (2018).
60. Torunbalci, M. M., Odelberg, T. J., Sridaran, S., Ruby, R. C. & Bhave, S. A. An FBAR circulator. *IEEE Microw. Compon. Lett* **28**, 395–397 (2018).
61. Yu, Y. et al. Highly-linear magnet-free microelectromechanical circulators. *IEEE J. Microelectromechanical Systems* **28**, 933–940 (2019).
62. Yu, Y. et al. Magnetic-free radio frequency circulator based on spatiotemporal commutation of MEMS resonators. In *Proc. IEEE Micro Electro Mech. Syst. (MEMS)* 154–157 (IEEE, 2018).
63. Xu, C. & Piazza, G. Magnet-less circulator using AlN mems filters and CMOS RF switches. *J. Microelectromech. Syst* **28**, 409–418 (2019).
64. Bahamonde, J., Kymissis, I., Alù, A. & Krishnaswamy, H. 1.95-GHz circulator based on a time-modulated electro-acoustic gyrator. In *Proc. IEEE Int. Symp. Antennas and Propagation and USNC-URSI Radio* (IEEE, 2018).
65. Ranzani, L. & Aumentado, J. Circulators at the quantum limit: recent realizations of quantum-limited superconducting circulators and related approaches. IEEE Microw. Mag. ***20***, 112–122 (2019).
66. Castellanos-Beltran, M. A. & Lehnert, K. W. Widely tunable parametric amplifier based on superconducting quantum interference device array resonator. *Appl. Phys. Lett.* **91**, 083509 (2007).
67. Josephson, B. D. Possible new effects in superconductive tunneling. *Phys. Lett.* **1**, 251–253 (1962).
68. Anderson, P. W. & Rowell, J. M. Probable observation of the Josephson superconducting tunneling effect. *Phys. Rev. Lett.* **10**, 230–232 (1963).
69. Abdo, B., Brink, M. & Chow, J. M. Gyrator operation using Josephson mixers. *Phys. Rev. Appl* **8**, 034009 (2017).
70. Abdo, B., Kamal, A. & Devoret, M. H. Nondegenerate three-wave mixing with the Josephson ring modulator. *Phys. Rev. B* **87**, 014508 (2013).
71. Lecocq, F. et al. Nonreciprocal microwave signal processing with a field-programmable Josephson amplifier. *Phys. Rev. Appl* **7**, 024028 (2017).
72. Sliwa, K. M. et al. Reconfigurable Josephson circulator/directional amplifier. *Phys. Rev. X* **5**, 041020 (2015).
73. Levy, C. S., Asbeck, P. M. & Buckwalter, J. F. A CMOS SOI stacked shunt switch with sub-500ps time constant and 19-Vpp breakdown. In 2013 IEEE Compound Semiconductor Intg. Circuit Symp. (CSICS) 1-4 (IEEE, 2013).
74. Hill, C., Levy, C. S., AlShammary, H., Hamza, A. & Buckwalter, J. F. RF watt-level low-insertion-loss high-bandwidth SOI CMOS switches. *IEEE Trans. Microw. Theory Tech.* **66**, 5724–5736 (2018).
75. Kazior, T.E. et al. High performance mixed signal and RF circuits enabled by the direct monolithic heterogeneous integration of GaN HEMTs and Si CMOS on a silicon substrate. In *2011 IEEE Compound Semiconductor Int. Circuit Symp. (CSICS)*, 1-4 (IEEE,2011).
76. Baraani Dastjerdi, M., Reiskarimian, N., Chen, T., Zussman, G. & Krishnaswamy, H. Full duplex circulator-receiver phased array employing self-interference cancellation via beamforming. 2018 IEEE Radio Freq. Int. Circuits Symp. (RFIC) 108–111 (IEEE, 2018).
77. Baraani Dastjerdi, M., Jain, S., Reiskarimian, N., Natarajan, A. & Krishnaswamy, H. Analysis and design of a full-duplex two-element MIMO circulator-receiver with high TX power handling exploiting MIMO RF and shared-delay baseband self-interference cancellation. *IEEE J. Solid State Circ* **54**, 3525–3540 (2019).
78. Serrano, D. C. et al. Nonreciprocal graphene devices and antennas based on spatiotemporal modulation. *IEEE Ant. Wireless Prop. Lett* **15**, 1529–1532 (2016).
79. Hadad, Y., Soric, J. C. & Alù, A. Breaking temporal symmetries for emission and absorption. *Proc. Natl Acad. Sci. USA* **113**, 3471–3475 (2016).
80. Taravati, S. & Caloz, C. Mixer-duplexer-antenna leaky-wave system based on periodic space-time modulation. *IEEE Trans. Ant. Prop* **65**, 442–452 (2017).
81. Tymchenko, M., Sounas, D. L., Nagulu, A., Krishnaswamy, H. & Alù, A. Quasielectrostatic wave propagation beyond the delay-bandwidth limit in switched networks. *Phys. Rev. X* **9**, 031015 (2019).
82. Fleury, R., Sounas, D. L. & Alù, A. Subwavelength ultrasonic circulator based on spatiotemporal modulation. *Phys. Rev. B* **91**, 174306 (2015).
83. Estep, N. A., Sounas, D. L. & Alù, A. Magnetless microwave circulators based on spatiotemporally modulated rings of coupled resonators. *IEEE Trans. Microw. Theory Tech* **64**, 502–518 (2016).
84. Soer, M. C. M., Klumperink, E. A. M., Boer, P. T. D., Vliet, F. E. V. & Nauta, B. Unified frequency-domain analysis of switched-series-RC passive mixers and samplers. *IEEE Trans. Circuits Syst. I* **57**, 2618–2631 (2010).
85. Reiskarimian, N., Zhou, J., Chuang, T. H. & Krishnaswamy, H. Analysis and design of two-port *N*-path bandpass filters with embedded phase shifting. *IEEE Trans. Circuits Syst. II* **63**, 728–732 (2016).
86. Hameed, S., Rachid, M., Daneshrad, B. & Pamarti, S. Frequency-domain analysis of *N*-path filters using conversion matrices. *IEEE Trans. Circuits Syst. II Express Briefs* **63**, 74–78 (2016).
87. Pavan, S. & Klumperink, E. A. M. Generalized analysis of high-order switch-RC *N*-path mixers/filters using the adjoint network. *IEEE Trans. Circuits Syst. I* **65**, 3267–3278 (2018).
88. Xu, C. & Piazza, G. A generalized model for linear periodically-time-variant circulators. *Sci. Rep* **9**, 8718 (2019).
89. Kane, C. L. & Mele, E. J. Z_2 topological order and the quantum spin Hall effect. *Phys. Rev. Lett.* **95**, 146802 (2005).
90. Qi, X.-L. & Zhang, S.-C. Topological insulators and superconductors. *Rev. Mod. Phys.* **83**, 1057 (2011).
91. Khanikaev, A. B., Fleury, R., Mousavi, S. H. & Alù, A. Topologically robust sound propagation in an angular-momentum-biased graphene-like resonator lattice. *Nat. Commun.* **6**, 8260 (2015).
92. Fleury, R., Khanikaev, A. B. & Alù, A. Floquet topological insulators for sound. *Nat. Commun.* **7**, 11744 (2016).
93. Haldane, F. D. M. & Raghu, S. Possible realization of directional optical waveguides in photonic crystals with broken time-reversal symmetry. *Phys. Rev. Lett.* **100**, 013904 (2008).
94. Yu, Z., Veronis, G., Wang, Z. & Fan, S. One-way electromagnetic waveguide formed at the interface between a plasmonic metal under a static magnetic field and a photonic crystal. *Phys. Rev. Lett.* **100**, 023902 (2008).
95. Wang, Z., Chong, Y., Joannopoulos, J. D. & Soljaćić, M. Observation of unidirectional backscattering-immune topological electromagnetic states. *Nature* **461**, 772–775 (2009).

Acknowledgements

This work was supported by the National Science Foundation, the Air Force Office of Scientific Research, and the Defense Advanced Research Projects Agency. We wish to thank T. Olsson and T. Hancock for useful feedback and comments.

Author contributions

A.N., N.R. and H.K. performed literature review and wrote the manuscript. H.K. directed and supervised the project.

Competing interests

The authors declare no competing interests.

Additional information

Correspondence should be addressed to H.K.